PHYSICAL REVIEW B VOLUME 48, NUMBER 23 15 DECEMBER 1993-I

Exciton relaxation and radiative recombination in semiconductor quantum dots

U. Bockelmann
Walter Schottky Institut, Technische Universität München, Am Coulombwall, D-85748 Garching, Germany
(Received 7 September 1993)

Radiative lifetimes and acoustic-phonon scattering times of near-band-gap excitons are calculated. With increasing spatial quantization, exciton relaxation by phonon emission decreases strongly in efficiency as compared to radiative recombination. A rate-equation analysis based on the calculated lifetimes indicates an increasing shift of the luminescence from the exciton ground state towards excited states. For typical parameters of dots fabricated from quantum wells the calculated total luminescence efficiency is not strongly reduced by the effect of a slowed relaxation. The luminescence from the ground state becomes weak for strong spatial quantization.

Optical spectroscopy of interband transitions is a powerful and widely used method in the study of low-dimensional semiconductor structures.[1] In quantum dots, also referred to as zero-dimensional (0D) systems, the charge carriers are confined in all three spatial directions. It has been demonstrated recently that inhomogeneous broadening, a serious problem in optical spectroscopy of artifical solid-state structures, can be avoided by microscopic spectroscopy of a single quantum dot.[2] The interpretation of the detailed experimental information that will be available by this technique requires an adequate theoretical description.

It has been shown theoretically that the atomiclike discrete energy spectrum strongly modifies electron-phonon scattering rates in quantum dots with respect to systems of higher dimensionality.[3] Efficient electron relaxation is possible only between levels which are separated by not more than a few meV (via LA-phonon emission) or by an energy within a few meV from the LO-phonon energy (via LO-phonon emission or via a two-phonon LO+LA scattering mechanism[4]). The experimental luminescence efficiency of 0D structures fabricated from quantum wells usually decreases by orders of magnitude with decreasing dot size. Benisty, Sotomayor-Torrès, and Weisbuch have pointed out that this could be an intrinsic effect related to the strong decrease of the electron LA-phonon scattering rates.[5] From a theoretical analysis which neglects excitonic effects, they have derived a decrease in luminescence efficiency comparable to the experimental results.

The theoretical work cited above is limited to the relaxation of single particles. Strictly speaking, the results can therefore only be applied to optical experiments at high carrier density, where the electron-hole Coulomb atttraction is efficiently screened. In this high-density regime, hot electrons in quantum dots are expected to relax efficiently by means of an Auger mechanism.[6] On the other hand, optical experiments are usually performed at low excitation intensity to get the best spectral resolution. At low carrier density excitonic effects are important.

In this paper we discuss energy states, relaxation, and radiative decay of near-band-gap excitons in quantum dots. A theoretical description is developed that is well suited for a comparison with 0D structures fabricated from narrow GaAs/$Al_xGa_{1-x}As$ quantum wells. The influence of the calculated relaxation and recombination rates on the continuous-wave (cw) luminescence is studied by means of a rate-equation analysis. The theoretical results are compared to microluminescence data from single GaAs quantum dots.[2]

Usually quantum dots are fabricated from quantum wells by a lateral patterning technique. In such structures the confinement related to the lateral potential is weak compared to that caused by the quantum-well potential. We construct the near-band-gap exciton states on the electron and heavy-hole ground subbands of the underlying quantum well. The neglection of heavy-hole–light-hole mixing and excited subbands is justified for near-band-gap excitons in quantum dots fabricated from narrow quantum wells. For the 30-Å-wide GaAs/$Ga_{0.7}Al_{0.3}As$ well basis used in this work, the 40-meV energy separation between the heavy-hole and light-hole grond subbands and the energies of excited subbands are large compared to the lateral confinement energies. The exciton envelope wave function is written

$$\Psi_{ex}(\mathbf{r}_e,\mathbf{r}_h)=\phi(x_e,y_e,x_h,y_h)\chi_e(z_e)\chi_h(z_h)\ , \tag{1}$$

where χ_e and χ_h are the quantum-well ground-state wave functions of the electron and heavy hole, respectively. The lateral envelope functions ϕ are solutions of the Hamiltonian:

$$H=H_0+H_{eh}\ ,$$

$$H_0=\sum_{\nu=e,h}\frac{-\hbar^2}{2m_\nu}\left[\frac{\partial^2}{\partial x_\nu^2}+\frac{\partial^2}{\partial y_\nu^2}\right]+\tfrac{1}{2}m_\nu\omega_\nu^2(x_\nu^2+y_\nu^2)\ , \tag{2}$$

$$H_{eh}=-\int\int dz_e dz_h|\chi_e(z_e)|^2|\chi_h(z_h)|^2\frac{e^2}{\varepsilon_l|\mathbf{r}_e-\mathbf{r}_h|}\ .$$

The lateral confinement is described by rotational-symmetric, parabolic potentials of different angular frequency for electrons and holes (ω_e and ω_h). For the lateral masses and the static dielectric constant we use the GaAs values $m_e=0.067m_0$, $m_h=0.11m_0$, and $\varepsilon_l=12.9$, where m_0 is the free-electron mass. The Hamiltonian H is diagonalized numerically by an expansion on the analytical eigenfunctions of H_0. The latter are products of solutions of a two-dimensional harmonic oscillator, characterized by the radial quantum numbers n_e,n_h (0,1,2,...) and the angular momentum quantum num-

 ©1993 The American Physical Society

bers l_e, l_h $(0, \pm 1, \pm 2, \ldots)$.[7] The symmetry of the problem with respect to rotations around the z axis implies the conservation of total angular momentum $j = l_e + l_h$. States of different j are decoupled. For each j value the 300 lowest energy basis states are used in the numerical calculation. The described development on a basis of noninteracting pair states has already been used in previous theoretical studies of quantum dot excitons.[8–12] These calculations have been focused on the binding energy and oscillator strength of radiative excitons (essentially on the ground state) and they do not consider nonradiative states or exciton-phonon scattering.

The radiative decay rate τ_0^{-1} of the exciton is calculated in the dipole approximation. We obtain the expression

$$\tau_0^{-1} = (8ne^2P^2E_{\rm ph}/3c^3\hbar^2)\left|\int d\mathbf{r}\,\psi_{\rm ex}(\mathbf{r},\mathbf{r})\right|^2 \quad (3)$$

which holds for heavy-hole and light-hole excitons in the diagonal approximation. In deriving Eq. (3), we have assumed a spatially constant refractive index ($n = 3.6$) and have performed an average over direction and polarization of the emitted photon. $E_{\rm ph}$ is the photon energy. For the Kane matrix element P we use $2m_0P^2 = 22.71$ eV. The integral in Eq. (3) is nonzero only for $j = 0$ excitons, as can be seen directly from the angular dependence of the basis functions.[7] This is not in contradiction to the $\Delta j = \pm 1$ selection rule for dipole transitions. Its validity is asured by the angular momentum of the periodic part of the exciton Bloch function.

In Fig. 1 numerical results for quantum dots based on a 30-Å-wide $GaAs/Ga_{0.7}Al_{0.3}As$ quantum well are presented. Assuming a fixed ratio ω_h/ω_e, we describe the lateral exciton confinement by $\hbar\omega_e$ alone. The used set of parameters corresponds to the experimental situation of Ref. 2. Length and position of the lines indicate the exciton inverse radiative lifetime and energy, respectively. Consequently, only radiative excitons appear in Fig. 1. For weak lateral confinement (e.g., $\hbar\omega_e = 1$ meV) we observe a series of equidistant levels with an inverse lifetime homogeneously decreasing with increasing energy and a few states of clearly longer radiative lifetime. In this weak lateral confinement limit, the exciton wave function can be written approximately as a product involving the electron-hole center of mass and relative coordinates separately. The equidistant lines evolve from the quantum-well s exciton by the parabolic quantization of the center-of-mass motion (ground state of the relative motion). The weakly radiative excitons involve excited states in the relative coordinate and originate from nonradiative 2D excitons. The energy positions and separations of the discrete exciton levels increase with $\hbar\omega_e$ and the center-of-mass and relative motion become increasingly coupled. States originating from nonradiative 2D excitons gain in oscillator strength while the radiative lifetime of the ground-state and first excited exciton increase significantly with lateral confinement. The latter is just the opposite of what would have been expected from the following, simple and widely used argument: The lateral potential confines electron and hole at the same spatial position and thus leads to an increase of the radiative

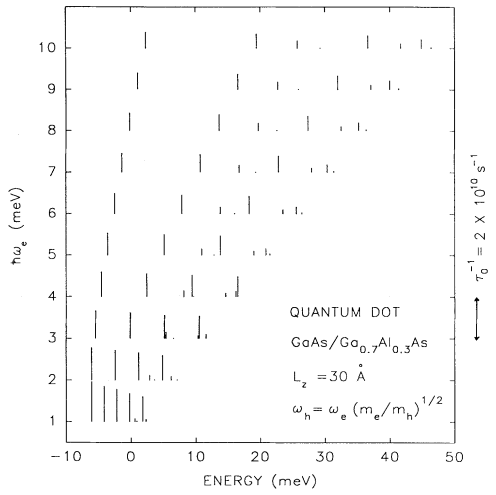

FIG. 1. Energy and inverse radiative lifetime τ_0^{-1} of the radiative excitons as a function of the confinement parameter $\hbar\omega_e$. The value of τ_0^{-1} is given by the length of the lines, in comparison to the double arrow on the right. Zero energy corresponds to the band gap of the underlying quantum well, namely, the sum of the bulk band gap and the confinement energies associated with $\chi_e(z)$ and $\chi_h(z)$.

recombination rate. However, this simple picture disregards the fact that the electron-hole pair is correlated even in the absence of lateral confinement. There exists a rough similarlity between the low-energy quantum dot exciton states discussed here and excitons bound to shallow impurities in bulk semiconductors. The oscillator strength of the latter exciton type has been studied some time ago by Rashba and Gurgenishvili[13] and by Henry and Nassau.[14] The latter authors conclude that the oscillator strength of the bound exciton is roughly given by the oscillator strength per unit cell of the free exciton, multiplied by the number of unit cells covered by the overlap of the electron and hole. The radiative lifetime is inverse proportional to the oscillator strength. The result obtained for impurity bound excitons thus agrees with our finding that in quantum dots the reduction of the spatial extension of the exciton wave function caused by the lateral confinement leads to an increased radiative lifetime. The same dependence has been found theoretically for the ground-state exciton of semiconductor microcrystals.[15,16]

Let us now turn to nonradiative lifetimes, namely, exciton-phonon scattering times that are calculated from the Fermi golden rule (phonon emission at zero temperature)

$$\tau_{i\to f}^{-1} = (2\pi/\hbar)\sum_{\mathbf{q}} |\langle \Psi_{\rm ex}^f | W | \Psi_{\rm ex}^i \rangle|^2 \delta(E_{\rm ex}^f - E_{\rm ex}^i + \hbar\omega_q)\ . \quad (4)$$

$E_{\rm ex}^i$, $E_{\rm ex}^f$, and $\hbar\omega_q$ are the energies of the exciton initial and final states and of the phonon of 3D wave vector $\mathbf{q}$, respectively. We calculate the scattering between the 0D excitons and bulk GaAs longitudinal-acoustic phonons, neglecting confinement effects on the phonon modes. The LA phonons are expected to give the dominant contibution to the relaxation of excitons of energy well below the optical-phonon branches ($\hbar\omega_{\rm LO}$ is about 36 meV in

GaAs). The LA-phonon dispersion is described by $\omega_q = c_s q$, with a longitudinal velocity of sound c_s of 3700 m/s. To derive the exciton-phonon interaction potential W we first determine the strain tensor associated with the phonon. The interaction potential is the sum of the strain-induced shift of the electron and the hole part of the exciton. The latter is obtained from the diagonal part of the Γ_8 strain Hamiltonian, originally derived by Pikus and Bir.[17] For heavy-hole excitons we obtain

$$W = \left[\frac{\hbar q}{2\rho_d c_s}\right]^{1/2} \left[D e^{i\mathbf{q}\cdot\mathbf{r}_e} + \left[\frac{l+m}{2} \frac{(q_x^2+q_y^2)}{q^2} + m\frac{q_z^2}{q^2} \right] e^{i\mathbf{q}\cdot\mathbf{r}_h} \right], \quad (5)$$

where ρ_d is the mass density, D the conduction-band de formation potential, and l,m are valence-band deformation potentials. We use $\rho_d = 5300$ kg/m^3, $D = 8.6$ eV, $l = 2.7$ eV, and $m = 8.7$ eV.

Figure 2 shows the dependence of the exciton relaxation rate τ_r^{-1} on the lateral confinement for two different radiative excitons. The quantity τ_r^{-1} is the sum over the scattering rates to all (radiative and nonradiative) exciton states of energy below the initial state. The complete spectrum of near-band-gap excitons is shown in Fig. 3, for the example of $\hbar\omega_e = 6$ meV. Scattering between any pair of exciton states is possible; there is no general selection rule. This contrasts to the case of phonon scattering between uncorrelated electron-hole pair states, where either the quantum numbers of the electron or the hole state have to be conserved. The contribution of a given transition is determined to a large extent by the energy separation of the involved levels which by energy conservation equals the phonon energy $\hbar\omega_q$. The exciton-phonon matrix element $\langle \Psi_{ex}^f | W | \Psi_{ex}^i \rangle$ first increases with $\hbar\omega_q$ due to the q-dependent prefactor in Eq. (5). Above a threshold energy of $\hbar c_s 2\pi/L_z$, however, the matrix element weakens considerably because of the increasingly rapid spatial oscillation of W caused by the harmonic exponentials. This implies that while relaxation of excitons at higher energy is efficient due to the small level spacings, the rate of transitions between the lowest exciton states strongly decrease with increasing lateral confinement. For $\hbar\omega_e$ above 2 meV the relaxation of the first excited $j=0$ state (solid line in Fig. 2) is dominated

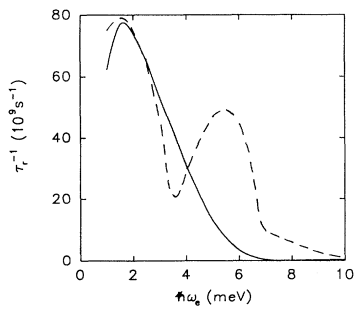

FIG. 2. Relaxation rate τ_r^{-1} of the first excited (solid line) and second excited (dashed line) $j=0$ excition as a function of lateral confinement at zero temperature.

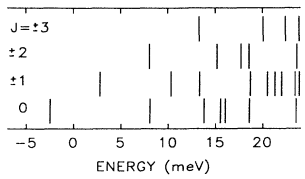

FIG. 3. Exciton energies of the $\hbar\omega_e = 6$ meV dot of Fig. 1, for different total angular momentum j.

by the transition to the $j=\pm1$ ground state. The homogeneous decrease reflects the increasing energy separation between these two levels. The result for the second excited $j=0$ state is more complicated (dashed line). While the overall decrease of τ_r^{-1} is again due to increasing energy-level separations, the additional strong structure between 3 and 7 meV indicates the importance of confinement-induced changes in the exciton envelope functions.

The cw photoluminescence of semiconductor structures is usually dominated by the exciton ground state since the relaxation of excited states is more efficient than their radiative decay. The comparsion of τ_0 and τ_r from Figs. 1 and 2 reveals that in 0D systems the relaxation rate of low-lying exciton states can be comparable or even smaller than the radiative recombination rate. The calculated exciton-phonon scattering and radiative recombination rates serve as ingredients in the following study of the quantum dot luminescence. A system of rate equations including all excitons below the third $j=0$ one is solved (all states below 15 meV in the case of Fig. 2). It contains phonon scattering between all levels, radiative decay (both calculated) and nonradiative decay (described by a phenomenological loss rate P, which is assumed to be the same for all levels). The restriction to the lowest states is justified by the fact that at higher energy the exciton spectrum is dense and therefore the exciton relaxation is efficient. The system is continuously pumped from the first states above it (one for each j value). The pump rates are given by the calculated phonon-scattering rates. We assume an equal occupation of all pump levels, sufficiently small to ensure that there are no state filling effects. In this way, a photoluminescence experiment with weak, continuous excitation is modeled.

Figure 4 shows the resulting intensitites of the three radiative excitons as a function of the nonradiative loss rate P. For zero P, all excitons pumped into the model system decay radiatively and the sum of the normalized intensities equals 1. The three figures represent different physical situations. If we consider single-particle relaxation, electrons and holes would relax efficiently in the 3-meV case; the hole would still relax efficiently but the electron would be hindered for $\hbar\omega_e = 6$ meV and at 10 meV relaxation of both carrier types would be slow with respect to radiative recombination. The excitonic analysis shows that for weak lateral confinment ($\hbar\omega_e = 3$ meV) the luminescence is dominated by the ground-state exciton, as is the case in 1D, 2D, or 3D systems. For intermediate $\hbar\omega_e$ (6 meV) the signals from the ground state and the excited states are important. This result is very interesting. It indicates that, in the absence of inhomogeneous broadening (single dot spectroscopy), excited states can

be studied by photoluminesence even at low excitation power. This is in agreement with the experimental results by Brunner *et al.*,[2] as will be discussed below. Usually arrays of quantum dots are investigated and the discrete transition peaks are covered by inhomogeneous broadening. There, the contribution of excited states would lead to a blueshift of the broadened luminescence peak which adds to the confinement induced one. The possibility of such a relaxation-induced blueshift should be kept in mind when an experimental shift is related to a mean structure size.

Until now, quantum dot structures fabricated from quantum wells belong to the case of weak or at most to the case of intermediate confinement of Fig. 4. The calculated total luminescence (the sum of the three intensities) decreases by less than a factor of 2 for nonradiative loss rates of up to 10^9 s^{-1}. This indicates that the experimentally observed, very strong decrease of the luminescence with decreasing quantum dot size is not mainly an effect of relaxation. Our exciton results are in striking contrast to the several orders of magnitude decrease in radiative efficiency that has been derived theoretically neglecting excitonic effects.[5]

For stronger lateral confinement (10 meV case of Fig. 4) exciton relaxation is slow and therefore the ground-state luminescence becomes very weak, already for small values of P. Whether the total luminescence is conserved by excited state luminescence or not, depends on whether the exciton is blocked on radiative (as in our analysis) or nonradiative levels. This will certainly depend on the detailed exciton sepctrum. Apart from that, the qualitative results of the analysis of luminescence are, to a large extent, independent of the details of the quantum dot structure.

Let us now compare the theoretical results with the luminescence data of Brunner *et al.*[2] The photoluminesce spectra measured from a series of single dots (Fig. 1 of Ref. 2) show roughly equidistant peaks reminiscent to our Fig. 1. The quantum dot of 450 nm geometrical size shows an experimental splitting of 10 meV between the ground and first excited transition and is therefore compared to the dot of $\hbar\omega_e = 6$ meV. In this case, the experimental intensity of the ground state and excited states are comparable, while for weaker lateral confinement the ground-state transition dominates. The former (latter) situation agrees with the 6-meV (3-meV) case of Fig. 4. The fine structure of the excited transitions of the 450-nm dot, which is particularly well

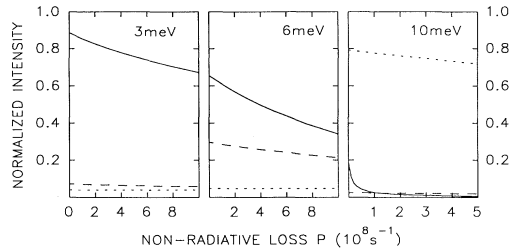

FIG. 4. Luminescence intensity from the ground state, first excited, and second excited radiative exciton (solid, dashed, and dotted line, respectively) for three different values of $\hbar\omega_e$.

resolved at low excitation power (Fig. 3 of Ref. 2), cannot be explained by the calculated spectrum of radiative excitons. However, Fig. 3 shows that the first excited radiative ($j=0$) state has almost the same energy as the lowest, twofold degenerate $j=\pm 2$ state. A deviation of the lateral potential from rotational symmetry would mix these three states, i.e., the nonradiative excitons would gain oscillator strength. This could be an explanation for the experimental fine structure consisting of three distinct peaks. The photoluminescence excitation spectrum collected from the ground-state transition of the 450-nm dot (curve PLE1 of Fig. 3 where PLE denotes photoluminescence excitation, Ref. 2) shows three small peaks between the luminenscence ground state and first excited state. This experimental structure cannot be assigned to calculated exciton levels.

In summary, relaxation and radiative recombination of quantum dot excitons have been studied theoretically. The radiative lifetime of excitons which derive from the ground state (excited states) of the relative coordinate increase (decrease) with increasing lateral confinement. Exciton-phonon scattering rates strongly decrease with increasing energy-level separation. For intermediate lateral quantization, the analysis of luminescence indicates the possibility of strong excited state transitions. For stronger confinement an increasingly inefficient relaxation by LA-phonon emission should lead to a very weak ground-state luminescence.

The author is grateful to G. Abstreiter, G. Bastard, K. Brunner, and P. Vogl for stimulating discussions. This work has been partly supported by the Deutsche Forschungsgemeinschaft (SFB348) and by a PROCOPE contract.

[1] C. Weissbuch and B. Vinter, *Quantum Semiconductor Structures: Fundamentals and Applications* (Academic, New York, 1991), and references cited therein.
[2] K. Brunner *et al.*, Phys. Rev. Lett. **69**, 3216 (1992).
[3] U. Bockelmann and G. Bastard, Phys. Rev. B **42**, 8947 (1990).
[4] T. Inoshita and H. Sakaki, Phys. Rev. B **46**, 7260 (1992).
[5] H. Benisty *et al.*, Phys. Rev. B **44**, 10 945 (1991).
[6] U. Bockelmann and T. Egeler, Phys. Rev. B **46**, 15 574 (1992).
[7] V. Fock, Z. Phys. **47**, 446 (1928).
[8] G. W. Bryant, Phys. Rev. B **37**, 8763 (1988).
[9] Y. Z. Hu *et al.*, Phys. Rev. B **42**, 1713 (1990).
[10] V. Halonen *et al.*, Phys. Rev. B **45**, 5980 (1992).
[11] W. Que, Phys. Rev. B **45**, 11 036 (1992).
[12] T. Takagahara, Phys. Rev. B **47**, 4569 (1993).
[13] É. I. Rashba and G. É. Gurgenishvili, Fiz. Tverd. Tela (Leningrad) **4**, 1029 (1962) [Sov. Phys. Solid State **4**, 759 (1962)].
[14] C. H. Henry and K. Nassau, Phys. Rev. B **1**, 1628 (1970).
[15] T. Takagahara, Phys. Rev. B **36**, 9293 (1987).
[16] E. Hanamura, Phys. Rev. B **37**, 1273 (1988).
[17] G. E. Pikus and G. L. Bir, Fiz. Tverd. Tela (Leningrad) **1**, 1502 (1959) [Sov. Phys. Solid State **1**, 1502 (1960)].